EAST EUROPEAN JOURNAL OF PHYSICS. **3.** 369-374 (2024)
DOI:10.26565/2312-4334-2024-3-44 ISSN 2312-4334

A COMPUTATIONAL INVESTIGATION ON THE STRUCTURAL, ELECTRONIC AND MAGNETIC PROPERTIES OF SI-DOPED $L1_0$-FENI ALLOY FOR CLEAN ENERGY

Zineb Zine[a,b], Nassima Meftah[b]*
[a]*LABTHOP Laboratory, Faculty of Exact Sciences, University of El-Oued, 3900 El-Oued, Algeria*
[b]*Department of physics, Faculty of Exact Sciences, University of El-Oued, 39000 El-Oued, Algeria*
**Corresponding Author e-mail: meftahnassima@yahoo.fr*
Received June 22, 2024; revised July 24, 2024; accepted August 8, 2024

For the first time, this study conducts a computational analysis by employing density functional theory (DFT) to investigate the effects of silicon doping as substitutional defects on the structural, electronic, and magnetic characteristics of the $L1_0$-FeNi alloy. The aim of this study was to explore the potential applications of Si-doped FeNi compounds as alternatives to rare-earth permanent magnets. For this, we have performed full potential calculations of $L1_0$-FeNi with substitutional Si-doping within a generalized gradient approximation. Two types of substitutional Si-doping (O_{Fe}/O_{Fe}) in the Ni/Fe site of the parent alloy have been investigated. The computed formation energy (E_f) indicates that the incorporation of silicon defects increases the structural stability of tetragonally distorted $L1_0$-FeNi. Moreover, our findings demonstrate that the FeNi:Si(O_{Ni}) in the $L1_0$-structure has a stable saturation magnetization (M_s), whereas the FeNi:Si (O_{Fe}) has a small reduction in M_s. Therefore, Si-substituted FeNi alloys can be tuned to become a good candidate for permanent magnets.
Keywords: *Ordered $L1_0$-FeNi; Density functional theory; Rare-earth free magnets; Substitutional defects*
PACS: 61.43.Bn, 71.15.Mb

INTRODUCTION

Permanent magnets have a significant role in many modern technologies, including electric motors, generators, sensors, and data storage devices [1,2]. These materials retain their magnetic characteristics even in the absence of an external magnetic field, making them ideal for a variety of applications. Permanent magnet performance is essentially governed by its magnetic characteristics, including coercivity, remanence, and maximal energy product [3, 4].

Rare-earth magnets, such as neodymium-iron-boron (NdFeB) and samarium-cobalt (SmCo), are the most powerful permanent magnets on the market today [5]. NdFeB magnets are well-known for their high magnetic strength and are commonly employed in applications that demand strong magnetic fields in small places, such as hard disk drives, electric vehicle motors, and wind turbines [6]. SmCo magnets, while somewhat less strong than NdFeB magnets, have higher temperature stability and corrosion resistance, making them ideal for high-temperature and harsh environmental applications [7]. However, research on permanent magnet materials is ongoing, with the goal of enhancing performance, lowering prices, and finding alternatives to rare-earth elements due to their scarcity and geopolitical difficulties. New alloy compositions, developments in production processes, and the research of hybrid materials that combine the greatest qualities of many types of magnets are all examples of innovation.

The ordered tetragonal FeNi alloy, commonly referred to as $L1_0$-FeNi or tetrataenite, is receiving widespread attention in the materials research community because of its promising magnetic characteristics, which are crucial for advanced technological applications [8, 9]. $L1_0$-FeNi has an arranged tetragonal structure, which contributes to its unusual magnetic characteristics [10]. Tetrataenite is found naturally in meteorites and formed by a highly slow cooling process of around 0.1 K per million years at 600 K [11, 12]. This gradual cooling allows the Fe and Ni atoms to organize themselves in a structured manner, resulting in the L_{10} phase, which consists of alternating layers of Fe and Ni. Maât *et al*. (2020) found that the ordered tetragonal FeNi alloy has strong saturation magnetization (M_s = 1.5 T), a high Curie temperature ($T_C \approx$ 830 K), and considerable magnetocrystalline anisotropy (MCA $\approx$ 1 MJ/m^3) [13]. These features make L_{10}-FeNi an appealing material for high-performance permanent magnets. However, while its MCA value is considerable, it is less than that required for optimal performance in permanent magnet applications [14]. Whereas, researchers have discovered several techniques, such as chemical vapor deposition, mechanical alloying and annealing, and electro-deposition, to synthesize $L1_0$-FeNi in the laboratory, as duplicating the natural gradual cooling process is impossible [15-17]. Defect engineering is now recognized as an important technique to improve the characteristics of $L1_0$-FeNi [18]. The introduction of controlled quantities of impurities or defects can have a major impact on the material's magnetic properties. Rani et al. (2019) discovered that substitutional platinum (Pt) doping cause tetragonal distortion, which boosts the MCA of $L1_0$-FeNi [19]. However, Pt doping is not cost-effective in large-scale applications. Furthermore, different techniques involve interstitial nitrogen (N) doping. Computational studies have demonstrated that N-doping can enhance the structural stability and MCA of tetragonally deformed FeNi, although with a minor decrease in saturation magnetization [20]. This method makes use of the strong bonding between nitrogen and the FeNi lattice to maintain the ordered structure and increase magnetic anisotropy.

Cite as: Z. Zine, N. Meftah, East Eur. J. Phys. 3, 369 (2024), https://doi.org/10.26565/2312-4334-2024-3-44

For the first time, this study investigated the effects of substitutional silicon doping on the structural, electronic, and magnetic properties of $L1_0$-FeNi alloys in order to improve their performance by using first-principles density functional theory (DFT) computational techniques. The substitutional silicon-doping was done at two separate sites: the Fe site (O_{Fe}) and the Ni site (O_{Ni}). However, the silicon atom was chosen for its size and chemical affinity for FeNi alloys.

COMPUTATIONAL METHODS

The $L1_0$-FeNi alloy has an AuCu-type tetragonal crystal structure with Fe and Ni layers that alternate along the c-axis. The $L1_0$-FeNi material has experimental lattice parameters a = 2.53 Å and c = 3.58 Å [21] and a crystal structure classified as P4/mmm. The supercells of FeNi with dimensions of 2×2×2 and 2×2×3 were considered to allow substitutional Si-doping at levels of 12.5% and 8.3%, respectively. To calculate the structural, electronic, and magnetic properties of pure FeNi and optimized Si-substituted FeNi, we use the full potential linearized augmented plane wave (FPLAPW) method, which is implemented in WIEN2k software [22], within the framework of density functional theory (DFT) [23]. To determine exchange-correlation energy, this study applied the spin-polarized Generalized Gradient Approximation (GGA) proposed by Perdew, Becke, and Ernzerhof (PBE) [24]. In FPLAPW calculations, the valence levels were considered scalar relativistically, but the core states were treated completely relativistically. Furthermore, the wave functions of valence electrons identified within the Muffin-Tin sphere have been substantially expanded, especially up to lmax = 10. The radius of the Muffin-Tin (RMT) spheres for each atom is selected so that they are almost touching, limiting charge leakage. $R_{MT}k_{max}$=7 was used to calculate the plane wave cut-off parameters, whereas Gmax was set to 12 a.u.$^{-1}$ for the Fourier expansion of potential in the interstitial area. The convergence criterion was set at 10^{-4} Ryd total energy. We employed the Monkhorst-pack technique in the Brillouin zone, with a 6x6x4 k-mesh.

RESULTS AND DISCUSSION

$L1_0$-FeNi crystal structure can be characterized by two types of unit cells: (i) face centered tetragonal (fct) and (ii) body centered tetragonal (bct); however, the bct, or primitive unit cell, will typically be chosen as the input structure for calculations due to its smallest basis and minimal computational cost [25]. Figure 1 depicts a 2×2×2 supercell of FeNi (bct) which stimulates 12.5% substitutional doping of Si by substituting one Ni atom with Si. Likewise, 8.3% Si-doping may be obtained in a 2×2×3 supercell.

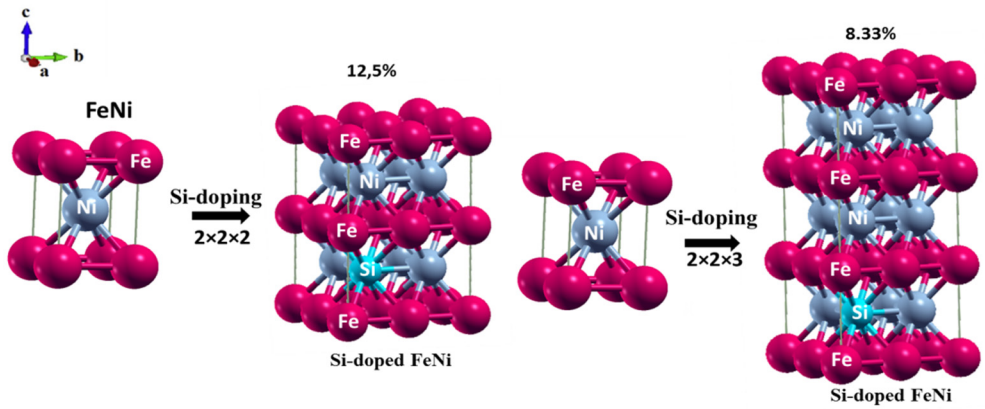

Figure 1. Front view of a 2×2×2 and 2×2×3 supercell of FeNi employed to simulate silicon-substitutional doping at 12.5% and 8.33% respectively

In order to get the ground state values of the lattice parameters (a and c) of FeNi and Si-doped FeNi alloys, we optimized the volume using L. D Marks' optimization approach [26].

The equilibrium lattice parameters and bulk modulus value for $L1_0$-FeNi and Si-doped $L1_0$-FeNi alloy were determined by fitting the total energy vs. volume data to the nonlinear Murnaghan equation of state [27], as shown in Fig. 2.

To examine the stability of the structure, the formation energy (E_{for}) of FeNi and FeNi:Si alloys was estimated using the prescribed formulae [19]:

$$E_{for}^{FeNi} = E_{FeNi} - E_{Fe} - E_{Ni}, \quad (1)$$

$$E_{for}^{FeNi-Si} = (E_{FeNi-Si} - \alpha E_{Fe} - \beta E_{Ni} - \gamma E_{Si}). \quad (2)$$

Where E_{FeNi}, $E_{FeNi\text{-}Si}$, E_{Fe}, E_{Ni}, and E_{Si} designate the ground state energies of pure FeNi, FeNi-Si supercells, and individual Fe, Ni, and Si atoms. However, α, β and γ represent the number of Fe, Ni, and Si atoms in the respective supercell.

The optimized lattice parameters (a and c), c/a ratio, formation energy, E_{For}/f.u. (eV), the bulk modulus B (GPa) and first order derivative of bulk modulus (B_0') of FeNi:Si alloys have been computed and are presented in Table 1. Our computed c/a ratio and formation energy for L_{10}-FeNi are consistent with previous findings for tetragonal ordered FeNi reported by Rani et al. (2019) [19]. As seen in Table 1, the c/a ratio increases with Si substitution, reflecting an increase in tetragonal distortion while keeping the area of the a-b plane roughly the same. The increased tetragonal distortion improves the structural stability of $L1_0$-FeNi, which is in accordance with the experimental findings published by Mizuguchi et al. (2011) [28]. As a result, we proved that substitutional silicon doping at either the Fe or Ni sites increases the stability of the $L1_0$-FeNi alloy. However, the negative values of formation energies (E_{For}) that were observed in each case are indicative of structural stability.

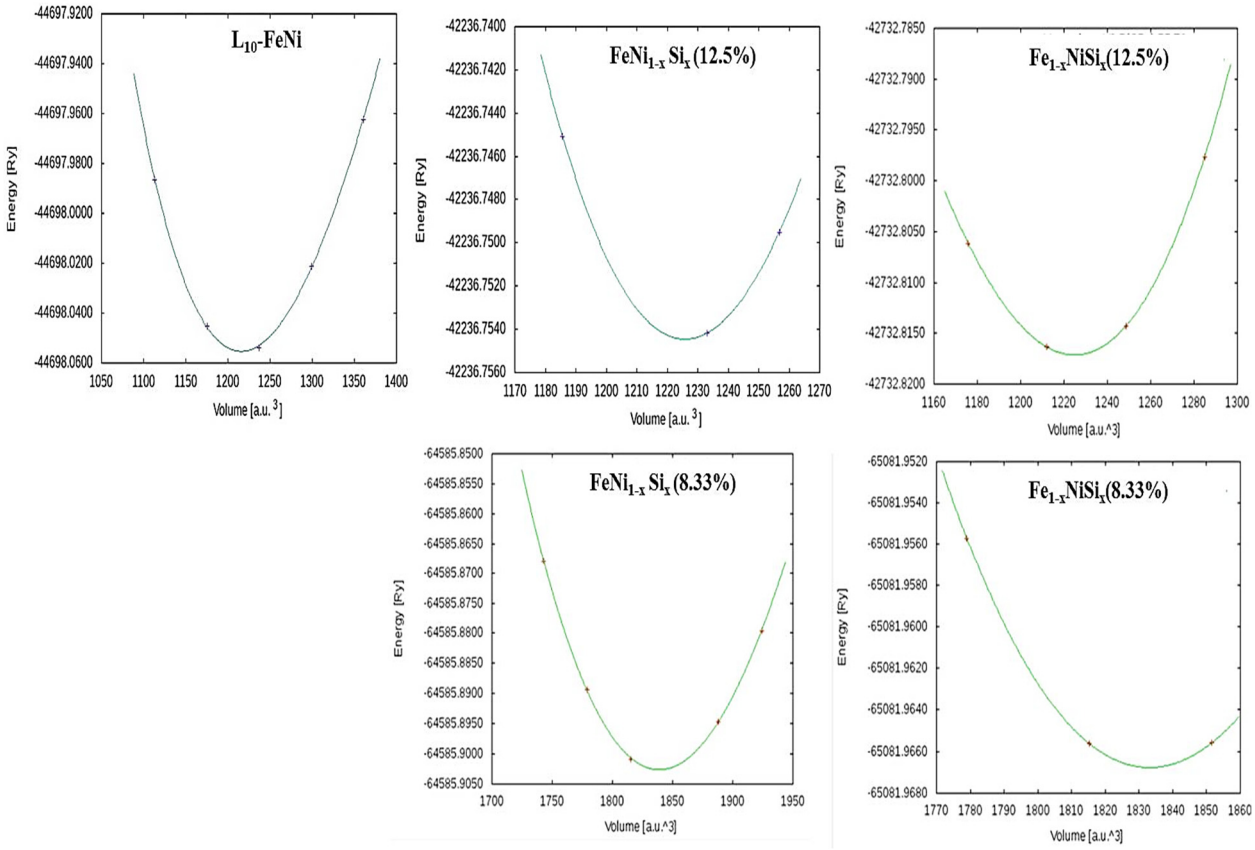

Figure 2: The total energy as a function of the volume of the compounds:
$L1_0$FeNi, $FeNi_{1-x}$ Si_x (12.5%), Fe_{1-x}Ni Si_x (12.5%), $FeNi_{1-x}$ Si_x (8.33%) and Fe_{1-x}Ni Si_x (8.33%)

Table 1. The optimized lattice parameters (a and c), tetragonal distortion (c/a), formation energy, E_{For}/f.u. (eV), the bulk modulus B (GPa) and first order derivative of bulk modulus (B_0') of $L1_0$- FeNi and Si doped FeNi compounds

Compound	**a(Å)**	**c(Å)**	**c/a**	**V(Å^3)**	**B(GPa)**	**B'$_0$**	**E_{For}/f.u**
FeNi (ref. [19])	2.531	3.579	1.414	22.93			− 0.18
FeNi (this work)	2.5140	3.562	1.417	22.51	197.828	4.763	− 0.181
$Fe_{1-x}NiSi_x$(12.5%)	2.5196	3.6059	1.4311	22.89	177.0856	6.01	− 0.027
$Fe_{1-x}NiSi_x$(8.33%)	2.5206	3.5778	1.4195	22.73	184.9932	4.0254	− 0.0283
$FeNi_{1-x}Si_x$(12.5%)	2.5181	3.6038	1.4311	22.85	195.8518	5.000	− 0.034
$FeNi_{1-x}Si_x$(8.33%)	2.5173	3.5815	1.4227	22.69	191.3532	5.000	− 0.0285

To investigate their electronic properties, Figure 3 shows the total and orbital projected density of states (DOS) for $L1_0$-FeNi, FeNi: Si (O_{Fe}), and FeNi: Si (O_{Ni}). The total DOS of all compounds appears highly spin polarized and metallic in nature. The fundamental electronic configurations of elements constituting pristine and Si-doped FeNi are Fe: [Ar] $4s^23d^6$, Ni: [Ar] $4s^23d^8$, and Si: $1s^22s^22p^63s^23p^2$, as represented in the projected electronic densities of states of all atoms. In pure FeNi, Fe-3d and Ni-3d hybridize thoroughly thereby contributing equally to total DOS. The fully filled 3d-orbitals of Fe and Ni in majority spin states are easily recorded, but in minority spin states, they are partly

occupied, resulting in high ferromagnetism for all compounds. On Si substitution, we see that hybridization between Fe-3d and Si-3p does not induce any significant shift in either the majority or minority spin states. The DOS in the vicinity of E_F are due to the admixture of Fe-3d/Ni-3d and Si-3p states.

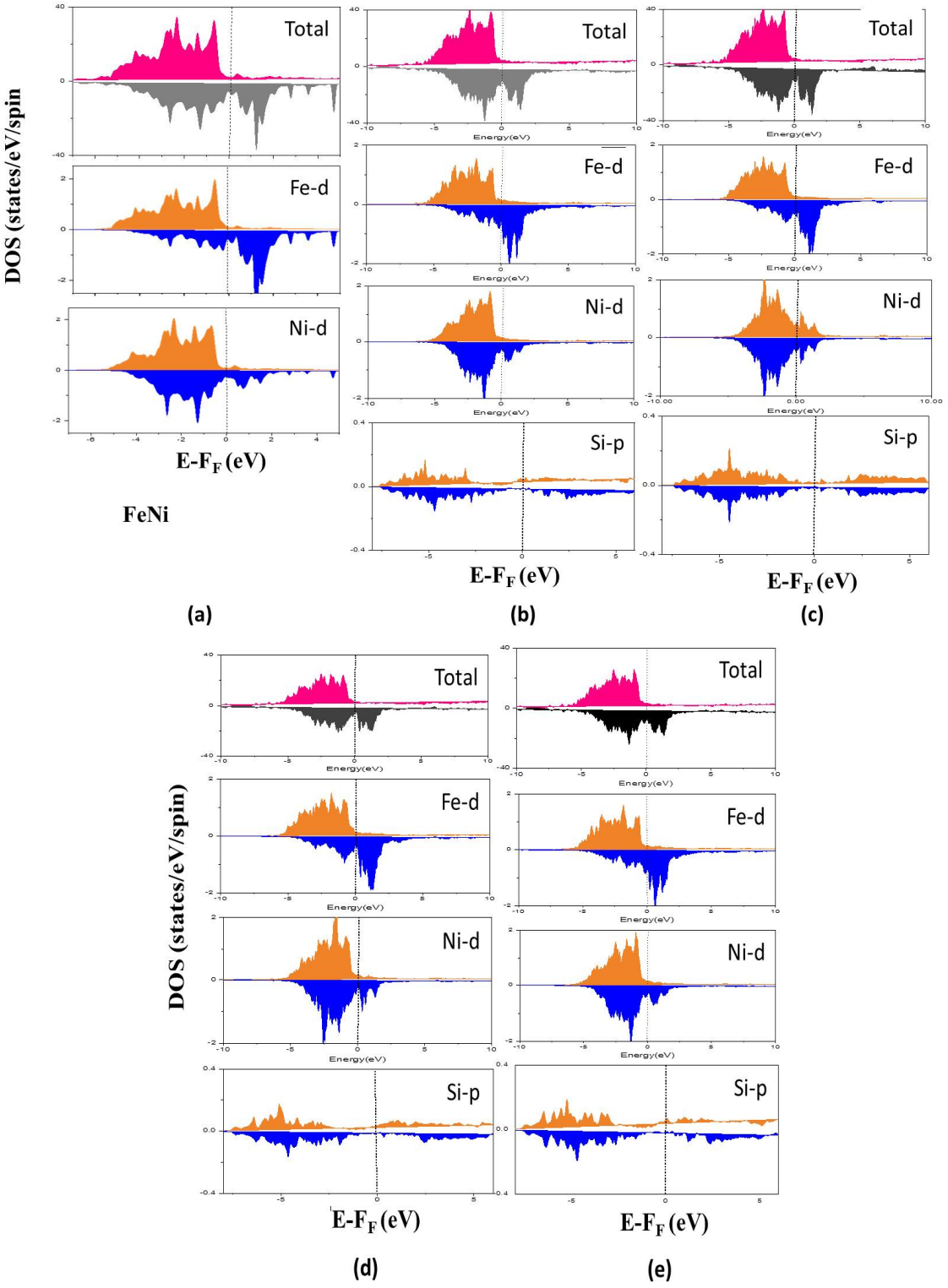

Figure 3. Computed total and projected density of states (DOS):
(a) FeNi, (b) $Fe_{1-x}NiSi_x$ (8.3%), (c) $FeNi_{1-x}Si_x$ (8.3%), (d) $Fe_{1-x}NiSi_x$ (12.5%) and (e) $FeNi_{1-x}Si_x$ (12.5%)

The difference between the majority and minority spin states in the occupied area may be used to determine the net magnetic moment. Table 2 displays the total atom-resolved spin magnetic moments as well as saturation magnetization (M_s) for pure and Si-doped FeNi alloys. According to the results, incorporating silicon affects the magnetic moments of the constituent atoms as well as the overall magnetic moment.

Table 2. Total and atom-resolved spin magnetic moments (μ_s), and saturation magnetization (M_s) of pure and Si-doped FeNi alloy.

Compounds	Magnetic Moments (μ_B)				M_s(T)
	Fe	Ni	Si	total	
FeNi (ref. [29])	2.701	0.645	/	3.272	1.33
FeNi (this work)	2.702	0.651	/	3.265	1.31
$Fe_{1-x}NiSi_x$(12.5%)	2.6717	0.6113	-0.0385	2.8190	1.14
Fe_{1-x} $NiSi_x$(8.33%)	2.6528	0.6531	-0.0315	2.9373	1.19
$FeNi_{1-x}Si_x$(12.5%)	2.6090	0.7086	-0.0673	3.0456	1.28
$FeNi_{1-x}Si_x$(8.33%)	2.7126	0.75027	-0.0688	3.1704	1.30

The minority spin states in Fe ($3d^6$) are less populated than in Ni ($3d^8$), resulting in a greater spin magnetic moment for Fe (2.7 μ_B) than Ni (0.65 μ_B). The decrease in the total spin magnetic moment of FeNi:Si (O_{Ni}/O_{Fe}) can be attributed to the phenomenon of hybridization between Ni-3d/Fe-3d states, in conjunction with the p-states of a non-magnetic impurity atom (Si-3p). This hybridization process leads to a reduction in the overall spin magnetic moment observed in the system. The decrease is more pronounced in FeNi:Si (O_{Fe}) due to antiparallel alignment of Si-3p with Fe-3d and Ni-3d states. All alloys have isotropic computed spin magnetic moments.

The saturation magnetization (M_s) is calculated as total spin magnetic moment per unit volume. As indicated in Table 2, the saturation magnetization of $L1_0$-FeNi is 1.31 T, which is almost equal to the previously computed theoretical value of 1.33 T [29, 30]. When Si substitutes into (O_{Fe}) in $L1_0$-FeNi alloy, the saturation magnetization Ms decreases from 1.31 T to 1.14 (1.19)T for FeNi:Si 12.5% (8.33%), and when Si is substituted into (O_{Ni}), the saturation magnetization M_s relatively decreases from 1.31 T to 1.28 (1.30)T for FeNi:Si 12.5% (8.33%). This reduce becomes more obvious in FeNi:Si(O_{Fe}) due to the decrease in Fe moment in the plane containing non-magnetic Si impurity. In addition, Fe is antiferromagnetically linked with the Si impurity in this case. Thus, the structural stability and magnetic properties clarify that out of two FeNi:Si alloys, FeNi:Si(O_{Ni}) 8.33% is more suitable candidate to act as permanent magnetic material.

CONCLUSIONS

We have studied the effect of doping the $L1_0$-FeNi binary alloy by introducing silicon (Si) atoms as a substitutional defect in the $L1_0$-bct structure. We have studied the structural, electronic and magnetic properties using the DFT from the first principle, as described above. Compared to the pristine FeNi alloy, we found that for FeNi:Si, the tetragonal distortion was increased, which yields the structural stability of these alloys. However, the saturation magnetization (M_s) was slightly reduced by the introduction of the Si atom, however, when the Si atom was substituted in the Ni site (8.33%), the saturation magnetization change was very small. Therefore, among those alloys, FeNi:Si (O_{Ni}) can be tuned to become a good candidate for permanent magnets, or the requirement for permanent magnets is achieved by this compound.

ORCID

Zineb Zine, https://orcid.org/0000-0001-8961-6220; **Nassima Meftah,** https://orcid.org/0000-0001-7646-8572

REFERENCES

[1] J. Ormerod, *Permanent magnet markets and applications. In Modern Permanent Magnets*, (Woodhead Publishing, 2022), pp. 403-434.
[2] A.H. King, and R.G. Eggert, *Critical materials for permanent magnets. In Modern Permanent Magnets*, (Woodhead Publishing, 2022), pp. 343-370.
[3] J.M.D. Coey, "Perspective and prospects for rare earth permanent magnets," Engineering, **6**(2), 119-131 (2020). https://doi.org/10.1016/j.eng.2018.11.034
[4] Z. Shao, and S. Ren, "Rare-earth-free magnetically hard ferrous materials," Nanoscale Adv. **2**(10), 4341-4349 (2020). https://doi.org/10.1039/D0NA00519C
[5] A. H. King, and R. G. Eggert, *Critical materials for permanent magnets. In Modern Permanent Magnets*, (Woodhead Publishing, 2022), pp. 343-370, https://doi.org/10.1016/B978-0-323-88658-1.00003-0
[6] H. Sepehri-Amin, S. Hirosawa, and K. Hono, "Advances in Nd-Fe-B based permanent magnets," in: *Handbook of magnetic materials*, **27**, 269-372 (2018). https://doi.org/10.1016/bs.hmm.2018.08.003
[7] O. Gutfleisch, M.A. Willard, E. Brück, C.H. Chen, S.G. Sankar, and J.P. Liu, "Magnetic materials and devices for the 21st century: stronger, lighter, and more energy efficient," Advanced materials. **23**(7), 821-842 (2011). https://doi.org/10.1002/adma.201002180
[8] S. Mandal, M. Debata, P. Sengupta, and S. Basu, "L_{10} FeNi: a promising material for next generation permanent magnets," Critical Reviews in Solid State and Materials Sciences, **48**(6), 703-725 (2023). https://doi.org/10.1080/10408436.2022.2107484
[9] T.Y. Tashiro, M. Mizuguchi, T. Kojima, T. Koganezawa, M. Kotsugi, T. Ohtsuki, and K. Takanashi, "Structural and magnetic properties of FeNi thin films fabricated on amorphous substrates," Journal of Applied Physics, **117**(17), 17E309 (2015). https://doi.org/10.1063/1.4913935
[10] S. Mandal, A. Panigrahi, A. Rath, M. Bönisch, P. Sengupta, M. Debata, and S. Basu, "Formation of $L1_0$ Ordering in FeNi by Mechanical Alloying and Field-Assisted Heat Treatment: Synchrotron XRD Studies," Acs Omega, **8**(15), 13690-13701 (2023). https://doi.org/10.1021/acsomega.2c07869
[11] E.R. Scott, "Iron meteorites: Composition, age, and origin," in: *Oxford Research Encyclopedia of Planetary Science*, (2020).

[12] N. Meftah, S. Mostefaoui, A. Jambon, E.H. Guedda, and S. Pont, "Minor and trace element concentrations in adjacent kamacite and taenite in the Krymka chondrite," Meteorit. Planet. Sci. **51**(4), 696-717 (2016). https://doi.org/10.1111/maps.12617
[13] N. Maât, I. McDonald, R. Barua, B. Lejeune, X. Zhang, G.M. Stephen, A. Fisher, *et al*., "Creating, probing and confirming tetragonality in bulk FeNi alloys," Acta Materialia, **196**, 776-789 (2020). https://doi.org/10.1016/j.actamat.2020.07.019
[14] Y. Miura, S. Ozaki, Y. Kuwahara, M. Tsujikawa, K. Abe, and M. Shirai, "The origin of perpendicular magneto-crystalline anisotropy in L_{10}–FeNi under tetragonal distortion," Journal of physics: Condensed matter, **25**(10), 106005 (2013), https://doi.org/10.1088/0953-8984/25/10/106005
[15] I.Z. Hlova, O. Dolotko, M. Abramchuk, A. Biswas, Y. Mudryk, and V.K. Pecharsky, "Enhancement of hard magnetism and chemical order of synthetic L_{10}-FeNi," J. Alloys Compd. **981**, 173619 (2024). https://doi.org/10.1016/j.jallcom.2024.173619
[16] S. Mandal, A. Panigrahi, A. Rath, M. Bönisch, P. Sengupta, M. Debata, and S. Basu, "Formation of $L1_0$ Ordering in FeNi by Mechanical Alloying and Field-Assisted Heat Treatment: Synchrotron XRD Studies," Acs Omega, **8**(15), 13690-13701 (2023). https://doi.org/10.1021/acsomega.2c07869
[17] F. Meneses, A. Pedernera, C. Blanco, N. Bajales, S.E. Urreta, and P.G. Bercoff, "$L1_0$-FeNi ordered phase in AC electrodeposited iron-nickel biphasic nanowires," Journal of Alloys and Compounds, **766**, 373-381 (2018). https://doi.org/10.1016/j.jallcom.2018.06.307
[18] M. Ali, and F. Ahmad, "A review of processing techniques for Fe-Ni soft magnetic materials," Materials and Manufacturing Processes, **34**(14), 1580-1604 (2019). https://doi.org/10.1080/10426914.2019.1662038
[19] P. Rani, J. Thakur, A. Taya, and M.K. Kashyap, "Magnetocrystalline anisotropy of Pt-doped $L1_0$-FeNi compound for clean energy applications," Vacuum, **159**, 186-190 (2019). https://doi.org/10.1016/j.vacuum.2018.10.023
[20] P. Manchanda, R. Skomski, N. Bordeaux, L.H. Lewis, and A. Kashyap, "Transitionmetal and metalloid substitutions in $L1_0$-ordered FeNi," J. Appl. Phys. **115**, 17A710 (2014). https://doi.org/10.1063/1.4862722
[21] P. Rani, R. Singla, J. Thakur, A.H. Reshak, and M.K. Kashyap, "Enhancement in magnetic parameters of $L1_0$-FeNi on Pd-substitution for permanent magnets," Indian J. Phys. **97**, 67–72 (2023). https://doi.org/10.1007/s12648-021-02221-y
[22] P. Blaha, K. Schwarz, G.K.H. Madsen, D. Kvasnicka, J. Luitz, R. Laskowski, F. Tran, and L.D. Marks, *WIEN2k an Augmented Plane Wave þ Local Orbitals Program for Calculating Crystal Properties, Revised Edition WIEN2k, 19.1*, (Vienna University of Technology, Vienna, Austria, 2019).
[23] M. Weinert, E. Wimmer, and A.J. Freeman, "Total-energy all-electron density functional method for bulk solids and surfaces," Phys. Rev. B, **26**, 4571 (1982). https://doi.org/10.1103/PhysRevB.26.4571
[24] J.P. Perdew, K. Burke, and M. Ernzerhof, "Generalized gradient approximation made simple," Phys. Rev. Lett. **77**, 3865 (1996). https://doi.org/10.1103/PhysRevLett.77.3865
[25] A. Edström, J. Chico, A. Jakobsson, A. Bergman, and J. Rusz, "Electronic structure and magnetic properties of $L1_0$ binary alloys," Physical Review B, **90**(1), 014402 (2014). https://doi.org/10.1103/PhysRevB.90.014402
[26] W. Marks, "Multicriteria optimisation of shape of energy-saving buildings," Building and environment, **32**(4), 331-339 (1997). https://doi.org/10.1016/S0360-1323(96)00065-0
[27] F.D. Murnaghan, "The compressibility of media under extreme pressures," Proceedings of the National Academy of Sciences, **30**(9), 244-247 (1944). https://doi.org/10.1073/pnas.30.9.24
[28] M. Mizuguchi, T. Kojima, M. Kotsugi, T. Koganezawa, K. Osaka, and K. Takanashi, "Artificial fabrication and order parameter estimation of L_{10}-ordered FeNi thin film grown on a AuNi buffer layer," Journal of the Magnetics Society of Japan, **35**(4), 370-373 (2011). https://doi.org/10.3379/msjmag.1106R008
[29] P. Rani, J. Thakur, A. Taya, and M. K. Kashyap, "Effect of tetragonal distortion induced by interstitial C-doping in $L1_0$-FeNi," AIP Conference Proceedings, **2115**(1), 030497 (2019). https://doi.org/10.1063/1.5113336
[30] E. Poirier, F.E. Pinkerton, R. Kubic, R.K. Mishra, N. Bordeaux, A. Mubarok, L.H. Lewis, *et al*., "Intrinsic magnetic properties of $L1_0$ FeNi obtained from meteorite NWA 6259," Appl. Phys. **117**, 17E318 (2015). https://doi.org/10.1063/1.4916190

ОБЧИСЛЮВАЛЬНЕ ДОСЛІДЖЕННЯ СТРУКТУРНИХ, ЕЛЕКТРОННИХ ТА МАГНІТНИХ ВЛАСТИВОСТЕЙ СПЛАВУ L1₀-FeNi, ЛЕГОВАНОГО Si ДЛЯ ЧИСТОЇ ЕНЕРГЕТИКИ

Зінеб Зіне[a,b], Нассіма Мефтах[b]

[a]*Лабораторія LABTHOP, Факультет точних наук, Університет Ель-Уед, 3900 Ель-Уед, Алжир*
[b]*Кафедра фізики, факультет точних наук, Університет Ель-Уед, 39000 Ель-Уед, Алжир*

У цьому дослідженні вперше проведено обчислювальний аналіз із застосуванням теорії функціоналу густини (DFT) для дослідження впливу легування кремнієм як дефектів заміщення на структурні, електронні та магнітні характеристики сплаву L1₀-FeNi. Мета цього дослідження полягала в тому, щоб вивчити потенційні можливості застосування легованих кремнієм сполук FeNi як альтернативи рідкоземельним постійним магнітам. Для цього ми виконали розрахунки повного потенціалу L1₀-FeNi із замісним легуванням кремнієм у межах узагальненого градієнтного наближення. Досліджено два типи замісного легування Si (O_{Fe}/O_{Fe}) у Ni/Fe місці вихідного сплаву. Обчислена енергія формування (E_f) вказує на те, що включення дефектів кремнію підвищує структурну стабільність тетрагонально спотвореного L1₀-FeNi. Крім того, наші результати демонструють, що FeNi:Si(O_{Ni}) у структурі L1₀ має стабільну намагніченість насичення (M_s), тоді як FeNi:Si(O_{Fe}) має невелике зниження M_s. Таким чином, Si-заміщені FeNi сплави можуть бути налаштованим, щоб стати хорошим кандидатом на постійні магніти.

Ключові слова: *впорядкований $L1_0$-FeNi; теорія функціонала густини; магніти без рідкоземельних елементів; дефекти заміни*